

The soft superconducting gap in semiconductor Majorana nanowires

So Takei, Benjamin Fregoso, Hoi-Yin Hui, Alejandro M. Lobos, and S. Das Sarma
*Condensed Matter Theory Center and Joint Quantum Institute, Department of Physics,
 University of Maryland, College Park, Maryland 20742-4111, USA.*

(Dated: April 8, 2022)

We theoretically consider the mysterious topic of the soft gap in the tunneling conductance of the proximity induced superconductivity in a semiconductor-superconductor hybrid structure, where the observation of a zero bias conductance peak has created considerable excitement because it could be connected with the existence of the elusive zero-energy Majorana mode. The observed experimental superconducting tunneling gap in the semiconductor nanowire looks v-shaped with considerable subgap conductance even at very low temperatures in sharp contrast to the theoretically expected hard BCS gap with exponentially suppressed subgap conductance. We systematically study, by solving the appropriate BdG equations both numerically and analytically, a number of physical mechanisms (e.g. magnetic and non-magnetic disorder, finite temperature, dissipative Cooper pair breaking, interface fluctuations), which could, in principle, lead to a soft gap, finding that only the interface fluctuation effect is a quantitatively and qualitatively viable mechanism that is consistent with the experimental observations. Our work indicates that improving the quality of the superconductor-semiconductor interface, so that the proximity tunneling amplitude is uniform along the semiconductor nanowire, would go a long way in enhancing the gap in the hybrid structures being used for studying the Majorana mode.

PACS numbers: 73.63.Nm, 74.45.+c, 74.81.-g, 03.65.Vf

Introduction. The pursuit of exotic topological phases of matter has become an exciting topic of research in physics [1]. In particular, topological superconductors (SCs) supporting zero-energy Majorana bound states (MBS) [2–13] have received increasing attention both for its intrinsic interest for fundamental physics as well as for its potential uses in topological quantum computation [2, 14–16]. In recent proposals to realize topological SCs in solid state systems, an effective p -wave SC is induced in a semiconductor by the combined effects of spin-orbit coupling (SOC), Zeeman splitting of the energy bands and proximity induced s -wave SC [8, 17, 18]. For a semiconductor nanowire (NW), it was predicted that the presence of MBS at its ends could be experimentally detected in the differential tunneling conductance $G(V) = dI/dV$ at the interface with a normal contact via the emergence of a zero-bias peak (ZBP) of height $2e^2/h$ (at zero temperature) [19–23]. Interestingly, recent experiments implementing the above NW proposal using InSb or InAs NWs in contact with a SC (mostly Nb) have shown a suggestive ZBP in the $G(V)$ spectra that is consistent with the theoretical predictions of the MBS scenario [24–26]. However, despite the enormous excitement generated by these results there are several discrepancies between theory and experiment that have attracted recent attention, e.g. the suppressed value of the ZBP compared with its predicted quantized Majorana value of $2e^2/h$ [27], the non-closing of the superconducting gap at the topological phase transition in the finite magnetic field [28], and the short wire length leading to possible Majorana overlap between the ends [29]. In addition, it has been pointed out that other mechanisms, notably disorder [30–33] and Kondo effect [34], could possibly lead to a ZBP in the experiments.

Curiously, an ubiquitous (and rather striking) feature of the experiment involving proximity-induced superconductivity in the semiconductor itself has remained ignored in the literature despite a great deal of activity in the subject: the supercon-

ducting gap in the NW, as reflected in the measured $G(V)$, is extremely “soft” in both the high-field topological phase (where the ZBP exists) and in the zero-field or the low-field trivial phase where there is no ZBP. In fact, the soft gap feature, which is clearly a property of the semiconductor-SC hybrid structure quite independent of the MBS physics, is extremely prominent in the data (even in the absence of the applied Zeeman field) with the subgap conductance being typically only a factor of 2-3 lower than the above-gap conductance, implying the existence of rather large amount of subgap states whose origin remains unclear. Amazingly, this soft gap issue has not been discussed at all in the theoretical literature, in spite of the soft gap being present in all of the experimental data from the groups so far appearing in the subject, and all the theoretical calculations invariably manifest the usual BCS hard gap (with the Majorana ZBP superposed on this hard gap above the magnetic-field-induced topological quantum phase transition). We believe that without a thorough understanding of this ubiquitous soft gap feature of the experiment the whole subject remains incomplete and even highly suspect.

In this Letter we provide the first theoretical attempt to explain the observed soft gap and perform a systematic theoretical investigation of different possible mechanisms giving rise to subgap tunneling conductance using a theoretical model similar to the experimental configurations in Refs. 24–26. In particular, we focus on the effects due to: (a) non-magnetic and (b) magnetic disorder in the NW; (c) temperature; (d) dissipative quasiparticle broadening arising due to various pair-breaking mechanisms such as poisoning, coupling to other degrees of freedom (e.g. phonons) or due to electron-electron interactions; and (e) inhomogeneities at the SC-NW interface due to imperfections (e.g. roughness and barrier fluctuations) that may arise during device fabrication. Since the soft gap occurs universally in the experiment at all parameter values, we consider only the non-topological zero-magnetic field situ-

ation in this paper because this is where the gap should be the largest and the hardest. Our results for the topological phase with finite magnetic field (not shown in this paper) are very similar qualitatively. Our numerical results point to a stronger effect of inhomogeneities at the semiconductor NW-SC interface (due to the exponential dependence on the barrier parameters), as compared to disorder, temperature or pair-breaking broadening effects, in producing the soft gap as described in the rest of this paper. We substantiate our numerical calculations with an analytical approach using Abrikosov-Gor'kov theory [35] within a minimal model for a semiconductor NW under the effect of a fluctuating s -wave pairing potential induced at the interface.

Theoretical model. We consider the Hamiltonian describing a narrow one-dimensional semiconductor NW of length L_x along the x -axis subject to SOC, Zeeman field along its axis, and proximity-induced s -wave pairing,

$$\hat{H}_w = \int_0^{L_x} dx \left\{ c_s^\dagger(x) \left[-\frac{\partial_x^2}{2m_e^*} - \mu(x) + i\alpha_R \sigma_y \partial_x - B_Z \sigma_x - \mathbf{b}(x) \cdot \boldsymbol{\sigma} \right] c_{s'}(x) + \Delta(x) \left(c_\uparrow^\dagger(x) c_\downarrow^\dagger(x) + \text{H.c.} \right) \right\}. \quad (1)$$

Here, $c_s^\dagger(x)$ creates an electron with spin projection $s = \uparrow, \downarrow$ at position x in the NW, m_e^* is the effective mass of the electrons in the semiconductor, α_R is the Rashba velocity related to the SOC energy $E_{so} = m_e^* \alpha_R^2 / 2$, B_Z is the Zeeman energy due to an external magnetic field along, $\boldsymbol{\sigma} = (\sigma_x, \sigma_y, \sigma_z)$ is the vector of Pauli matrices, and $\Delta(x)$ is the (fluctuating) proximity-induced s -wave SC pairing. The sums over spin indices are implied. Static non-magnetic disorder in the semiconductor NW is included through a fluctuating chemical potential $\mu(x) = \mu_0 + \delta\mu(x)$ around the average value μ_0 . Static magnetic disorder may be present in the sample due to contamination with magnetic atoms or due to the presence of regions in the NW acting as quantum dots with an odd number of electrons. Assuming that the experimental temperature T is higher than the Kondo temperature T_K associated with the magnetic impurities, we can neglect the quantum dynamics of the impurity spins and model its effect as a randomly oriented inhomogeneous magnetic field $\mathbf{b}(x)$ [36]. Finally, we also introduce spatial (and associated potential) fluctuations in the barrier separating the NW and the SC. These fluctuations give rise to spatial fluctuations in the proximity-induced s -wave SC pairing in the NW. The induced pairing is very well approximated by the relation $\Delta(x) = \gamma(x) \Delta_{SC} / (\gamma(x) + \Delta_{SC})$, where Δ_{SC} is the uniform parent pairing in the bulk SC, and $\gamma(x) = \rho_0 t_\perp^2(x)$ is the transparency of the NW-SC interface [37]. Here, ρ_0 is the local density of states of electrons in the NW at the Fermi energy in the normal phase, and $t_\perp(x)$ is the tunneling matrix element connecting the SC and NW. The effect of the interface inhomogeneities is modeled through $t_\perp(x) = t_\perp^0 e^{-\kappa \delta d(x)}$, where $\delta d(x)$ denotes the fluctuation in the width of the NW-SC barrier and κ is a phenomenological constant with units of inverse length that parametrizes the energy barrier of the NW-SC interface. Such a functional form is expected due to

fluctuations in the overlap of evanescent wavefunctions. For $\gamma(x) \ll \Delta_{SC}$, the induced SC pairing is controlled by the interface transparency $\Delta(x) \approx \gamma(x)$ [37], and thus can be modeled as $\Delta(x) = \Delta_0 e^{-2\delta\beta(x)}$, where the dimensionless parameter $\delta\beta(x) = \kappa \delta d(x)$ characterizes the roughness of the interface, and Δ_0 is the induced SC pairing in the absence of the interface inhomogeneity. Note that our model for interface fluctuations is generic and only incorporates the invariable presence of pairing potential fluctuations at the interface separating the SC metal and the NW. A good interface by definition will have very little fluctuations whereas a poor interface will have large fluctuations.

We approximate (1) by a tight-binding Hamiltonian defined on an N_x -site lattice,

$$\begin{aligned} \hat{H}_w = & -t \sum_{\langle ij \rangle} c_{is}^\dagger c_{js} + i\alpha \sum_i \left[c_{is}^\dagger \sigma_{ss'}^y (c_{i+1s'} - c_{i-1s'}) \right] \\ & - \sum_i c_{is}^\dagger [\mu_0 + \delta\mu_i - B_Z \sigma^x - \mathbf{b}_i \cdot \boldsymbol{\sigma}] c_{is'} \\ & + [\Delta_i c_{i\uparrow}^\dagger c_{i\downarrow}^\dagger + \text{H.c.}], \end{aligned} \quad (2)$$

where $\alpha = \alpha_R / 2a$, and a is the lattice constant. The estimated parameters for the InSb NW are $L_x = 2\mu\text{m}$, $m_e^* = 0.015m_e$, $E_{so} = m_e^* \alpha_R^2 / 2 = 50\mu\text{eV}$, $\Delta_0 = 250\mu\text{eV}$, and temperature $T = 70\text{mK} \approx 0.024\Delta_0$ [24]. For our tight-binding simulations we use a one-band model with $N_x = 500$, $t = 676\mu\text{eV}$, and $\alpha = 0.07t$. The different disorder mechanisms are taken into account by introducing Gaussian-distributed random variables $\delta\mu_i$, $\mathbf{b}_i = (b_i^x, b_i^y, b_i^z)$, and $\delta\beta_i$ with zero mean and variance given by $\langle \delta\mu_i \delta\mu_j \rangle = W_\mu^2 \delta_{ij}$, $\langle b_i^p b_j^q \rangle = W_b^2 \delta_{ij} \delta_{pq}$, and $\langle \delta\beta_i \delta\beta_j \rangle = W_\beta^2 \delta_{ij}$, respectively. To model the interface inhomogeneity, we coarse-grain the interface in patches of length $5a$ and assume that $\delta\beta_i$ is uniform within each patch, but varies randomly from patch to patch with a standard deviation of W_β . Note that assuming a Gaussian distribution in $\delta\beta_i$ results in a different probability distribution function for Δ_i ,

$$P(\Delta_i) = \frac{1}{2\Delta_i \sqrt{2\pi} W_\beta} \exp \left[-\frac{1}{8W_\beta^2} \ln^2 \left(\frac{\Delta_i}{\Delta_0} \right) \right], \quad (3)$$

from which the mean $\langle \Delta_i \rangle = \int_0^\infty d\Delta_i P(\Delta_i) \Delta_i$ and variance $W_\Delta^2 = \int_0^\infty d\Delta_i P(\Delta_i) (\Delta_i - \langle \Delta_i \rangle)^2$ are calculated. For example a typical variation of 10% in the width of the barrier, i.e. $W_\beta = 0.1$, causes a variation $W_\Delta / \langle \Delta_i \rangle \approx 0.2$ in the s -wave pairing.

The relevant experimental quantity is the tunneling differential conductance $G(V)$ at an end of the NW, which is related to the local density of states [24, 25]. We calculate $G(V)$ using the tunneling formalism by coupling the NW to a contact lead [21, 22, 38]. The Hamiltonian of the combined system is $\hat{H} = \hat{H}_w + \hat{H}_L + \hat{H}_t$, where $\hat{H}_L = \sum_{ks} \epsilon_k d_{ks}^\dagger d_{ks}$ is the Hamiltonian describing the lead and $\hat{H}_t = t_L \sum_{ks} d_{ks}^\dagger c_{1s} + \text{H.c.}$ is the tunneling Hamiltonian coupling site $i = 1$ of the NW to the lead via a tunneling matrix element t_L . The tunneling conductance at the site $i = 1$ is then

$$G(V, T) = -2\pi e^2 t_L^2 \rho_L \int_{-\infty}^{\infty} d\omega \rho_1^w(\omega) f'(\omega - eV), \quad (4)$$

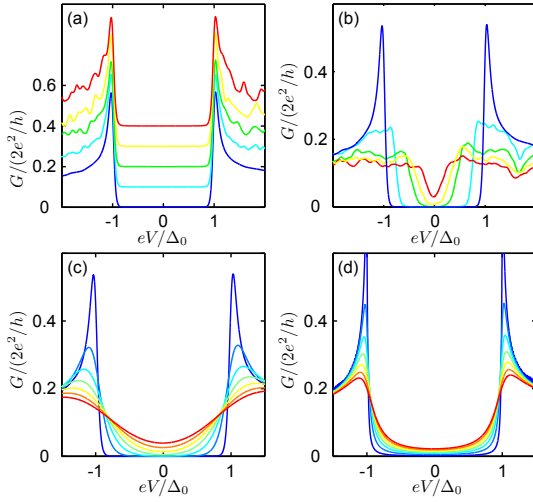


FIG. 1: (color online) Differential conductance for electron tunneling into an end of the semiconductor nanowire for zero external magnetic field. Various possible scenarios for subgap states are considered: (a) static disorder, (b) magnetic disorder, (c) thermal pair-breaking scenario and (d) quasiparticle broadening scenario. See text for more details.

where $f(x) = (e^{x/T} + 1)^{-1}$ is the Fermi distribution function, ρ_L is the density of states at the Fermi energy in the lead, and V is the voltage at which the lead is biased with respect to μ_0 . Here, $\rho_1^w(\omega)$ is the local density of states in the NW (including both spin projections) at site $i = 1$ in the presence of the lead, which we calculate as $\rho_1^w(\omega) = -\frac{1}{\pi} \text{Im} g_{11}^w(\omega)$. Here $g_{ij}^w(\omega)$ is the retarded Green's function of the NW in real-space representation, which in the limit $t_L \rightarrow 0$ becomes

$$g_{ij}^w(\omega) = \sum_{ns} \frac{u_{is,n}^{(0)*} u_{js,n}^{(0)}}{\omega - E_n^{(0)} + i\gamma_{L,n}} + \frac{v_{is,n}^{(0)*} v_{js,n}^{(0)}}{\omega + E_n^{(0)} + i\gamma_{L,n}}, \quad (5)$$

with $E_n^{(0)}$ and $\{u_{is,n}^{(0)}, v_{is,n}^{(0)}\}$ being, respectively, the eigenvalues and eigenvectors resulting from the diagonalization of the BdG Hamiltonian corresponding to Eq. (2). To include the presence of the lead, we solved the equation of motion for $g_{ij}^w(z)$ in the presence of the tunneling term \hat{H}_t [39]. The term $\gamma_{L,n}$ is the self-energy, which in the limit $t_L \rightarrow 0$ becomes $\gamma_{L,n} = -i\pi\rho_L t_L^2 \sum_s (|u_{1s,n}^{(0)}|^2 + |v_{1s,n}^{(0)}|^2)$.

Results. We now present the numerical results for $G(V)$. A mean chemical potential of $\mu_0 = -338\mu\text{eV}$ is used, and the temperature is set to $T = 70\text{mK}$ [24] unless otherwise stated. In Fig. 1(a) we consider the effect of static disorder on $G(V)$. We take $W_b = 0$ (blue curve) to $W_b = 0.8\Delta_0$ (red curve) in equal steps of $0.2\Delta_0$. The plots are offset in steps of $0.1 \times 2e^2/h$ for clarity. As expected from Anderson's theorem [36, 40], our results show that the subgap density of states is not affected by the presence of static non-magnetic disorder, thus rendering this an unlikely mechanism for the observed subgap conductance. We note as an aside that in our numerical results for the topological phase, which are not shown here, the effect of non-magnetic disorder is stronger than in

the zero magnetic field non-topological phase since Anderson's theorem does not apply in the topological phase. In fact, the non-magnetic disorder in the topological phase behaves very similar to the magnetic disorder in the non-topological phase discussed below.

The effect of magnetic disorder is shown in Fig. 1(b). We have taken $W_b = 0, 0.27\Delta_0, 0.54\Delta_0, 0.68\Delta_0$ and $0.81\Delta_0$ (blue to red curves). In this case, we find a substantial modification in the subgap conductance. In particular, a soft superconducting gap, similar to the one observed in Ref. 24, is obtained for $W_b = 0.81\Delta_0$ (red curve). Although we cannot exclude the presence of magnetic disorder, a large amount is needed to explain the data. We obtain $\Delta_0\tau_b \sim 1$, where $\tau_b = 2t^2(1 - (\mu/2t)^2)/3v_F W_b^2$ is estimated from our tight binding parameters. Such a large amount of magnetic disorder is unlikely to be present in the NW used in the experiments.

The thermal pair-breaking effect is considered in Fig. 1(c). Note that in our non-interacting theoretical description, thermal effects can only arise from broadening of the Fermi distribution function in Eq. (4). We vary the temperature from $T = 0.027\Delta_0$ (blue curve) to $T = 0.35\Delta_0$ (red curve) in equal steps of $0.054\Delta_0$ (the conversion is $0.027\Delta_0 \approx 78\text{mK}$). Although a considerable amount of thermally-induced subgap conductance is obtained for $T = 0.35\Delta_0$ (red curve), this value is much larger than the reported experimental temperature $T_{\text{exp}} = 70\text{mK}$, and cannot by itself explain the experimental features. We note that the blue curve corresponds to $T = 78\text{mK} \gtrsim T_{\text{exp}}$, for which there is no appreciable subgap conductance.

In Fig. 1(d), we consider the effect of a finite quasiparticle broadening due to dissipative processes. While it is experimentally unclear what physical mechanism would give rise to this broadening, it can in principle arise due to coupling of electrons in the NW to a source of dissipation, e.g. presence of (unconsidered) normal contacts, quasiparticle poisoning due to tunneling of normal electrons into the NW, scattering with phonons and/or other electrons. These pair-breaking mechanisms can be phenomenologically modeled by a shift in the frequency $\omega \rightarrow \omega + i\gamma_N$ in Eq. (5), where γ_N is the quasiparticle broadening. Quasiparticle lifetime effects were considered in a similar way in the context of BCS superconductors by introducing a phenomenologically broadened density of states $\rho(\omega, \gamma_N) = \text{Re}[(|\omega| + i\gamma_N)/(|\omega| + i\gamma_N)^2 + \Delta_0^2]^{1/2}$ [41]. In Fig. 1(d) we vary γ_N from $\gamma_N = 0.027\Delta_0$ (blue curve) to $\gamma_N = 0.35\Delta_0$ (red curve) in equal steps of $0.054\Delta_0$. We see that even for the largest values of γ_N (i.e. $\gamma_N \sim 0.35\Delta_0$ corresponding to the red curve), a remnant of the hard SC gap is still present. Therefore, this effect alone is incapable of explaining the substantial gap softening observed in the experiments.

While all of the above-mentioned mechanisms are likely to be present to some extent in a realistic setup, our results indicate that it is unlikely that they can individually explain the experimentally observed soft gap. Moreover, even after combining all the effects of non-magnetic and magnetic disorder, quasiparticle decay rate of order $0.1\Delta_0$, and temperature of 70mK , we found that obtaining a soft gap that qualitatively

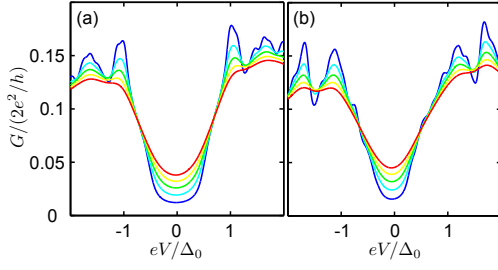


FIG. 2: (color online) Differential tunneling conductance for zero external magnetic field in the presence of SC-NW interface disorder and quasiparticle broadening. Two different interface inhomogeneity strengths are taken: (a) $W_\beta = 0.4$ and (b) $W_\beta = 0.8$. In each plot, we consider quasiparticle decay rates from $\gamma_N = 0.11\Delta_0$ (blue curve) to $\gamma_N = 0.32\Delta_0$ (red curve) in equal steps of $0.054\Delta_0$. See text for more details.

agrees with experiments requires magnetic disorder strength of $\Delta_0\tau_b \sim \mathcal{O}(1)$, which seems to be unrealistic. This leads us finally to the effect of inhomogeneities at the NW-SC interface (see Fig. 2). More generically, pair-breaking mechanisms at the interface have also been put forward to explain the transport properties in other semiconductor-SC systems that show similar subgap conductance [42]. We now argue that a reasonable amount of interface inhomogeneity together with quasiparticle broadening gives a soft gap that is in good qualitative and semi-quantitative agreement with the experimental findings, thus rendering the combination of these two effects as the most likely candidate for the soft gap. In Fig. 2, we take (a) $W_\beta = 0.4$ and (b) $W_\beta = 0.8$. In each plot, the five curves correspond to γ_N varying from $\gamma_N = 0.11\Delta_0$ (blue curve) to $\gamma_N = 0.32\Delta_0$ (red curve), in equal steps of $0.054\Delta_0$. We observe a large amount of subgap contributions, with a noticeable “v-shaped” tunneling conductance around $V = 0$, which is consistent with experimental observations [24, 25]. In Fig. 2(b), we see that $\gamma_N \sim 0.1\Delta_0$ is sufficient to obtain a soft gap reminiscent of the experimental findings.

An order-of-magnitude estimate for the dimensionless parameter $\delta\beta_i$ can be obtained based on known experimental parameters. The width of the NWs used in Ref. 24 was quoted as $100\text{nm} \pm 10\text{nm}$. Assuming that the fluctuations in the SC-NW barrier width is of order the wire width fluctuations, we take $\delta d_i \approx 5\text{nm}$. The phenomenological barrier parameter κ can be estimated using the interface energy barrier U_0 via $\kappa \approx \sqrt{2m_e^*U_0}/\hbar$. Using an estimate for U_0 based on a Nb-InGaAs junction [43], we take $U_0 \approx 0.2\text{ eV}$. With an effective mass for the InSb wire, $m_e^* \approx 0.015m_e$, we obtain $\delta\beta_i \sim 1$. This order of magnitude estimate is consistent with the standard deviations $W_\beta = 0.4$ and 0.8 used in this work.

A minimal analytical model that captures the relevant effects can be obtained from Eq. (1) in the absence SOC, Zeeman effect and other types of disorder, and assuming the SC pairing *itself* to be a Gaussian variable $\Delta(x) = \Delta_0 + \delta\Delta(x)$ with variance $\langle \delta\Delta(x)\delta\Delta(x') \rangle = W_\Delta^2\delta(x-x')$. This model allows one to obtain a useful insight into the effects of a fluctuating SC pairing on $G(V)$. We use the theoretical framework of the

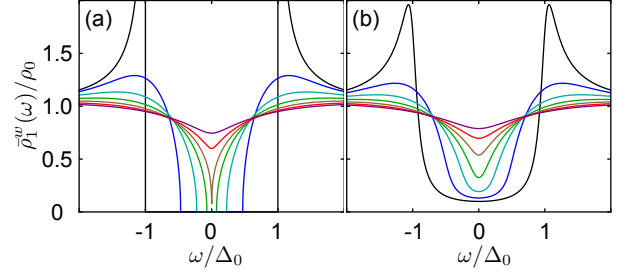


FIG. 3: (color online) Analytical results for $\bar{\rho}_1^w(\omega)/\rho_0$, the averaged local density of states obtained from the self-consistent Abrikosov-Gor’kov for various values of $\Delta_0\tau_\Delta$, and (a) $\gamma_N = 0$ and (b) $\gamma_N = 0.11\Delta_0$. See text for more details.

self-consistent Abrikosov-Gor’kov theory [35, 36] to obtain the *averaged* electron Green’s function $\bar{g}_{ij}^w(\omega)$. The calculations are shown in detail in the supplementary material [44]. Despite the mathematical similarity of the formalism to the (more usual) case of scattering induced by magnetic impurities in *s*-wave SCs, here we are only considering SC pairing fluctuations as the pair-breaking mechanism. In Fig. 3(a), we show the results for $\bar{\rho}_1^w(\omega)/\rho_0$, the averaged local density of states at the end of the NW, which is the main quantity determining $G(V)$ at $T = 0$ [cf. Eq. (4)]. In each plot, the black to purple curves correspond to $(\Delta_0\tau_\Delta)^{-1} = 0$ to 1.5 in equal steps of 0.25 . Here, $\tau_\Delta^{-1} \equiv \pi W_\Delta^2\rho_0$ is the scattering rate induced by SC pairing fluctuations. Interestingly, the theory allows us to obtain an analytical expression for the quasiparticle gap spectrum in $\bar{\rho}_1^w(\omega)/\rho_0$: $E_{\text{gap}} = \Delta_0[1 - (\Delta_0\tau_\Delta)^{-2/3}]^{3/2}$ [44]. For $\Delta_0\tau_\Delta \leq 1$, the quasiparticle gap vanishes (brown curve). To make contact with our numerical results in Fig. 2, in Fig. 3(b) we consider a finite $\gamma_N = 0.11\Delta_0$, for the same values of $\Delta_0\tau_\Delta$ as in Fig. 3(a). The quasiparticle decay rate γ_N has the effect of broadening the sharp edge features present in the tunneling spectrum when $\gamma_N = 0$. Again, we see that fluctuations in the induced SC pairing together with quasiparticle broadening gives the characteristic v-shaped tunneling spectrum in the subgap regime (e.g. cyan and green curves). Despite the minimal nature of our analytical model, the theory qualitatively explains the results of our numerical simulations.

To summarize, we have studied the effect of different pair-breaking mechanisms likely arising in semiconductor-SC Majorana NWs, and systematically analyzed their influence on the subgap tunneling conductance in order to explain the experimentally observed soft gap behavior. While we cannot completely rule out some of these mechanisms (i.e. magnetic scattering, thermal and dissipative broadening), quantitative considerations point to the interface fluctuations at the semiconductor-SC contact leading to inhomogeneous pairing amplitude along the wire as the primary physical mechanism causing the ubiquitous soft gap behavior. Our work indicates that materials improvement leading to optimized semiconductor-SC interfaces should considerably ameliorate the proximity gap in the hybrid structures.

Acknowledgments. The authors are grateful to Meng Cheng

and Claudia Ojeda-Aristizabal for valuable discussions. We acknowledge support from DARPA QuEST, JQI-NSF-PFC and Microsoft Q.

-
- [1] A. Kitaev, Usp. Fiz. Nauk **171**, 131 (2001), supplement; Proceedinds of Chernoglovka 2000, cond-mat/001440.
 - [2] C. Nayak, S. H. Simon, A. Stern, M. Freedman, and S. Das Sarma, Rev. Mod. Phys. **80**, 1083 (2008).
 - [3] S. Das Sarma, C. Nayak, and S. Tewari, Phys. Rev. B **73**, 220502 (2006).
 - [4] S. Tewari, S. D. Sarma, C. Nayak, C. Zhang, and P. Zoller, Phys. Rev. Lett. **98**, 010506 (2007).
 - [5] L. Fu and C. L. Kane, Phys. Rev. Lett. **100**, 096407 (2008).
 - [6] C. Zhang, S. Tewari, R. M. Lutchyn, and S. Das Sarma, Phys. Rev. Lett. **101**, 160401 (2008).
 - [7] M. Sato and S. Fujimoto, Phys. Rev. B **79**, 094504 (2009).
 - [8] J. D. Sau, R. M. Lutchyn, S. Tewari, and S. Das Sarma, Phys. Rev. Lett. **104**, 040502 (2010).
 - [9] R. M. Lutchyn, J. D. Sau, and S. Das Sarma, Phys. Rev. Lett. **105**, 077001 (2010).
 - [10] Y. Oreg, G. Refael, and F. von Oppen, Phys. Rev. Lett. **105**, 177002 (2010).
 - [11] J. Alicea, Phys. Rev. B **81**, 125318 (2010).
 - [12] L. Jiang, T. Kitagawa, J. Alicea, A. R. Akhmerov, D. Pekker, G. Refael, J. I. Cirac, E. Demler, M. D. Lukin, and P. Zoller, Phys. Rev. Lett. **106**, 220402 (2011).
 - [13] L. P. Rokhinson, X. Liu, and J. K. Furdyna, 10.1038/nphys2429.
 - [14] J. D. Sau, S. Tewari, and S. Das Sarma, Phys. Rev. A **82**, 052322 (2010).
 - [15] J. Alicea, Y. Oreg, G. Refael, F. von Oppen and M. P. A. Fisher, Nature Physics **7**, 412 (2011).
 - [16] B. van Heck, A. R. Akhmerov, F. Hassler, M. Burrello, and C. W. J. Beenakker, New J. Phys. **14** 035019 (2012).
 - [17] R. M. Lutchyn, J. D. Sau, and S. Das Sarma, Phys. Rev. Lett. **105**, 077001 (2010).
 - [18] Y. Oreg, G. Refael, and F. von Oppen, Phys. Rev. Lett. **105**, 177002 (2010).
 - [19] K. Sengupta, I. Žutić, H.-J. Kwon, V. M. Yakovenko, and S. Das Sarma, Phys. Rev. B **63**, 144531 (2001).
 - [20] K. T. Law, P. A. Lee, and T. K. Ng, Phys. Rev. Lett. **103**, 237001 (2009).
 - [21] J. D. Sau, S. Tewari, R. M. Lutchyn, T. D. Stanescu, and S. Das Sarma, Phys. Rev. B **82**, 214509 (2010).
 - [22] K. Flensberg, Phys. Rev. B **82**, 180516 (2010).
 - [23] M. Wimmer, A. R. Akhmerov, J. P. Dahlhaus, and C. W. J. Beenakker, New J. Phys. **13**, 053016 (2011).
 - [24] V. Mourik, K. Zuo, S. M. Frolov, S. Plissard, E. A. Bakkers, and L. Kouwenhoven, Science **336**, 1003 (2012).
 - [25] A. Das, Y. Ronen, Y. Most, Y. Oreg, M. Heiblum, and H. Shtrikman, ArXiv e-prints (2012), 1205.7073.
 - [26] C. M. Marcus, private communication.
 - [27] C.-H. Lin, J. D. Sau, and S. Das Sarma, ArXiv e-prints (2012), 1204.3085.
 - [28] T. D. Stanescu, R. M. Lutchyn, and S. Das Sarma, ArXiv e-prints (2012), 1208.4136.
 - [29] T. D. Stanescu, S. Tewari, J. D. Sau, and S. Das Sarma, ArXiv e-prints (2012), 1206.0013.
 - [30] D. Bagrets and A. Altland (2012), arXiv:1206.0434.
 - [31] J. Liu, A. C. Potter, K. Law, and P. A. Lee (2012), arXiv:1206.1276.
 - [32] D. I. Pikulin, J. P. Dahlhaus, M. Wimmer, H. Schomerus, and C. W. J. Beenakker (2012), arXiv:1206.6687.
 - [33] G. Kells, D. Meidan, and P. W. Brouwer (2012), arXiv:1207.3067.
 - [34] E. J. H. Lee, X. Jiang, R. Aguado, G. Katsaros, C. M. Lieber, and S. De Franceschi, Phys. Rev. Lett. **109**, 186802 (2012).
 - [35] A. A. Abrikosov and L. P. Gor'kov, Zh. Eksp. Teo. Fiz. **39**, 1781 (1960).
 - [36] A. V. Balatsky, I. Vekhter, and J.-X. Zhu, Rev. Mod. Phys. **78**, 373 (2006).
 - [37] T. D. Stanescu, R. M. Lutchyn, and S. Das Sarma, Phys. Rev. B **84**, 144522 (2011).
 - [38] Y. Meir and N. S. Wingreen, Phys. Rev. Lett. **68**, 2512 (1992).
 - [39] G. D. Mahan, *Many-Particle Physics*, Physics of Solids and Liquids (Kluwer Academic/Plenum Publishers, New York, 2000), 3rd ed.
 - [40] P. W. Anderson, J. Phys. Chem. Solids **11**, 26 (1959).
 - [41] R. C. Dynes, V. Narayanamurti, and J. P. Garno, Phys. Rev. Lett. **41**, 1509 (1978).
 - [42] K. Neurohr, A. A. Golubov, T. Klocke, J. Kaufmann, T. Schäpers, J. Appenzeller, D. Uhlisch, A. V. Ustinov, M. Hollfelder, H. Lüth, et al., Phys. Rev. B **54**, 17018 (1996).
 - [43] A. Kastalsky, A. W. Kleinsasser, L. H. Greene, R. Bhat, F. P. Milliken, and J. P. Harbison, Phys. Rev. Lett. **67**, 3026 (1991).
 - [44] See Supplemental Material for detailed calculations.

Appendix: Supplemental Materials for “The soft superconducting gap in semiconductor Majorana nanowires”

In this supplementary document we present the details of the Abrikosov-Gor'kov theory [1] adapted to handle pairing potential fluctuations.

Let us consider the Dyson's equation for the Green function in the presence of fluctuating pairing potential:

$$G_{kk'} = G_k^{(0)} \delta_{kk'} + \sum_p G_k^{(0)} V_{kp} G_p^{(0)} G_{k'}^{(0)} + \sum_p G_k^{(0)} V_{kp} G_p^{(0)} V_{pk'} G_{k'}^{(0)} \quad (\text{A.1})$$

$$+ \sum_{pp'} G_k^{(0)} V_{kp} G_p^{(0)} V_{pp'} G_{p'}^{(0)} V_{p'k'} G_{k'}^{(0)} + \dots \quad (\text{A.2})$$

where $G_k^{(0)} = (z\tau_0 - \xi_k\tau_3 - \Delta_0\tau_1)^{-1}$ is the Green function for the superconducting wire with uniform Δ_0 , and $V_{kp} = (\delta\Delta)_{k+p}\tau_1$ is the fluctuation in pairing potential. τ_i are the Pauli matrices acting on the particle-hole space. If we consider a Gaussian white noise for Δ_0 :

$$\langle \delta\Delta_k \rangle = 0 \quad (\text{A.3})$$

$$\langle \delta\Delta_k \delta\Delta_{k'} \rangle = W_\Delta^2 \delta_{k,-k'} \quad (\text{A.4})$$

then the fluctuation-averaged Green function can be evaluated with cumulant expansion:

$$\begin{aligned} \bar{G}_k \delta_{kk'} &= G_k^{(0)} \delta_{kk'} + \sum_p G_k^{(0)} \tau_1 G_p^{(0)} \tau_1 G_{k'}^{(0)} \langle \delta\Delta_{kp} \delta\Delta_{pk'} \rangle \\ &+ \sum_{pp'} G_k^{(0)} \tau_1 G_p^{(0)} \tau_1 G_{p'}^{(0)} \tau_1 G_{p'}^{(0)} \tau_1 G_{k'}^{(0)} \\ &\times \langle \delta\Delta_{kp} \delta\Delta_{pp'} \delta\Delta_{p'p''} \delta\Delta_{p''k'} \rangle + \dots \end{aligned} \quad (\text{A.5})$$

$$\begin{aligned} \bar{G}_k &= G_k^{(0)} + W_\Delta^2 G_k^{(0)} \tau_1 \left(\sum_p G_p^{(0)} \right) \tau_1 G_k^{(0)} \\ &+ W_\Delta^4 G_k^{(0)} \tau_1 \left(\sum_p G_p^{(0)} \right) \tau_1 G_k^{(0)} \tau_1 \left(\sum_p G_p^{(0)} \right) \tau_1 G_k^{(0)} \\ &+ W_\Delta^4 G_k^{(0)} \tau_1 \left(\sum_{pp'} G_p^{(0)} \tau_1 G_{p'}^{(0)} \tau_1 G_{p'}^{(0)} \right) \tau_1 G_k^{(0)} \\ &+ W_\Delta^4 G_k^{(0)} \tau_1 \left(\sum_{pp'} G_p^{(0)} \tau_1 G_{p'}^{(0)} \tau_1 G_{k+p'-p}^{(0)} \right) \tau_1 G_k^{(0)} \\ &+ \dots \\ &\equiv G_k^{(0)} + G_k^{(0)} \Sigma_k \bar{G}_k \end{aligned} \quad (\text{A.6})$$

Note that this expression is formally exact, provided we include all higher order processes. We now consider the following approximation for the self-energy: $\Sigma_k = W_\Delta^2 \int \frac{dp}{2\pi} \tau_1 \bar{G}_p \tau_1$. This corresponds to the “non-crossing approximation” where terms like $\sum_{pp'} G_p^{(0)} \tau_1 G_{p'}^{(0)} \tau_1 G_{k+p'-p}^{(0)}$ are ignored. This is a good approximation if $k_F v_F \tau_\Delta \gg 1$, where $\tau_\Delta^{-1} = \pi W_\Delta^2 \rho_0$ is

the scattering rate and ρ_0 is the density of states at the Fermi point for the wire with uniform Δ .

For notational convenience we rewrite the fluctuation-averaged Green function as

$$\begin{aligned} \bar{G}_k &= (z\tau_0 - \xi_k\tau_3 - \Delta_0\tau_1 - \Sigma)^{-1} \\ &= (\tilde{z}\tau_0 - \tilde{\xi}_k\tau_3 - \tilde{\Delta}\tau_1)^{-1} \end{aligned} \quad (\text{A.7})$$

where $\tilde{z} = z - \Sigma_0$, $\tilde{\xi}_k = \xi_k + \Sigma_3$ and $\tilde{\Delta} = \Delta_0 + \Sigma_1$. Here the self-energy is split into its components: $\Sigma = \Sigma_0\tau_0 + \Sigma_3\tau_3 + \Sigma_1\tau_1$.

The self-energy can be readily evaluated as

$$\begin{aligned} \Sigma_k &= W_\Delta^2 \int \frac{dp}{2\pi} \frac{\tilde{z} + \tilde{\xi}_k\tau_3 + \tilde{\Delta}\tau_1}{\tilde{z}^2 - \tilde{\xi}_k^2 - \tilde{\Delta}^2} \\ &= \frac{-1}{2\tau_\Delta} \frac{\tilde{z} + \tilde{\Delta}\tau_1}{\sqrt{\tilde{\Delta}^2 - \tilde{z}^2}} \end{aligned} \quad (\text{A.8})$$

Substituting this expression into Eq. (A.7) yields the renormalization of the energy and pairing potential:

$$\tilde{z} = z + \frac{1}{2\tau_\Delta} \frac{\tilde{z}}{\sqrt{\tilde{\Delta}^2 - \tilde{z}^2}} \quad (\text{A.9})$$

$$\tilde{\Delta} = \Delta_0 - \frac{1}{2\tau_\Delta} \frac{\tilde{\Delta}}{\sqrt{\tilde{\Delta}^2 - \tilde{z}^2}} \quad (\text{A.10})$$

The density of states in the presence of pairing potential fluctuation is obtained by

$$\begin{aligned} \rho(\epsilon) &= \frac{-1}{\pi} \text{Im} \int \frac{dk}{2\pi} \text{Tr} \bar{G}_k(z \rightarrow \epsilon + i0) \\ &\approx \rho_0 \text{Im} \frac{u}{\sqrt{1-u^2}} \\ &= \rho_0 (\Delta_0 \tau_\Delta) \text{Im} u \end{aligned} \quad (\text{A.11})$$

where we have defined $u \equiv \tilde{z}/\tilde{\Delta}$ and the relation $\frac{z}{\Delta_0} = u \left(1 - \frac{(\Delta_0 \tau_\Delta)^{-1}}{(1-u^2)^{1/2}} \right)$ is used in the last step. The gap in the quasi-particle spectrum is the smallest ω at which u acquires an imaginary part. For the function $z(u)$ for real u , the maximum value of z , beyond which u becomes complex, is [2]:

$$E_{\text{gap}} = \theta(\Delta_0 \tau_\Delta - 1) \Delta_0 \left(1 - (\Delta_0 \tau_\Delta)^{-2/3} \right)^{3/2} \quad (\text{A.12})$$

To compute the local density of states near the end of a semi-infinite wire, we add an impurity at $r = 0$ of an infinite wire: $V_{\text{imp}} = U\delta(r)\tau_3$. Taking the limit $U \rightarrow \infty$ will cut the wire into two halves. Consider now the Dyson's equation for the fluctuation-averaged Green function in the presence of the impurity:

$$\begin{aligned} \bar{G}_{\text{imp}}(r, r) &= \bar{G}(r, r) + \bar{G}(0, r) U \tau_3 \bar{G}_{\text{imp}}(0, r) \\ \bar{G}_{\text{imp}}(0, r) &= \bar{G}(0, r) + \bar{G}(0, 0) U \tau_3 \bar{G}_{\text{imp}}(0, r) \\ &= \left[1 - \bar{G}(0, 0) U \tau_3 \right]^{-1} \bar{G}(0, r) \\ \therefore \bar{G}_{\text{imp}}(r, r) &= \bar{G}(0) + \bar{G}(r) \tau_3 \left[U^{-1} - \bar{G}(0) \tau_3 \right]^{-1} \bar{G}(-r) \end{aligned}$$

where $\bar{G}(r) = \int \frac{dk}{2\pi} e^{ikr} \bar{G}_k$. Hence the Green function in the presence of a boundary is $\bar{G}_b(r, r) = \bar{G}_{\text{imp}}(r, r)|_{U \rightarrow \infty} = \bar{G}(0) - \bar{G}(r) \bar{G}(0)^{-1} \bar{G}(-r)$. The local density of states at r is then $\frac{-1}{\pi} \text{ImTr} \bar{G}_b(r, r)$.

[2] K. Maki in *Superconductivity* ed by R. D. Parks, Marcel Dekker, New York, 1969, v.2, p.1035.

[1] A. A. Abrikosov and L. P. Gor'kov, Zh. Eksp. Teo. Fiz. **39**, 1781 (1960).